Domain Decomposition for a Linear Advection-Diffusion Equation by means of minimax filtering

Emanuele Ragnoli[†], Sergiy Zhuk[†], Mykhaylo Zayats[‡] and Michael Hartnett[‡]
[†] IBM Research, Dublin, Ireland, [‡] NUIG Galway
eragnoli@ie.ibm.com

***Abstract*— In this work a novel strategy that combines Domain Decomposition, Differential Algebraic Equations (DAE) and Minimax Estimation is created to contruct a numerical solution for a linear non stationary advection-diffusion equation. The proposed approach helps to control the error introduced by Domain Decomposition and FEM discretisation and allows to combine observations with solutions of the advection-diffusion equation.**

I. Introduction

Forecasting sediment flows and pollution run-off in coastal and marine zones is done in geophysiscs with a combination of numerical models and data from sensors. Since this is categorised as a pollutant transport phenomenon it is usually modelled by a linear advection-diffusion equation with non-stationary coefficients which represent a fluid flow that in realistic situations is considered nonstationary. Thus, for the numerical transport model, one needs to take into account non-stationarity in the inflow and outflow zones on the boundary of the domain. This makes it impossible to a priori prescribe correct boundary conditions at the inflow and outflow zones. On the other hand, the choice of incorrect boundary conditions could lead to a so called boundary layer deteriorations, affecting the accuracy of the numerical model. These issues are usually overcome in two different ways: a sufficiently dense network of sensors is deployed to accurately measure the concentration of a pollutant on the boundary; the numerical domain is chosen to be large enough to guarantee zero concentrations at the boundaries. The latter is the solution of choice in the civil engineering practice but, over large physical domains, can quickly lead to very expensive computational schemes. A traditional way of overcoming the computational burden is by using Domain Decomposition ([8]). A novel strategy that combines Domain Decomposition (DD), Differential Algebraic Equations (DAE) and Minimax Estimation approach to solve this problem is proposed in this work. In more details, the original problem is decomposed into sub-problems assigned to related subdomains. The set of subproblems is then recasted as a DAE and sensors readings are used to detect the location of pollutants concentrations. Then the actual computation takes place only over those subdomains where the concentration of a pollutant is above zero. In particular, the subdomain gets activated/deactivate once the concentration reaches/leaves the boundaries of that subdomain. The exchange of information between the subdomains is carried out by the minimax filter.

This paper is organised as follows: section I-A lists the motivations for this work and describes related work; section I-B contains notations; section II contains the problem statement and discusses a Global Problem and Decomposed Problem obtained via DD section II-B describes the discretization with Finite Elements and the relations between the Discretised Global Problem and Discretised Decomposed Problem; section III elaborates on a minimax state estimation and introduces the approach; section IV presents numerical experiments, and, finally, section V contains the Conclusions.

A. Motivation and Related Work

Domain Decomposition is an approach for the numerical solution of partial differential equations. The set of methods that are grouped under it consists of the use of different numerical schemes within different subdomains of the domain representing a large scale problem. Such techniques have several advantages: the computational cost can be optimally managed, different geometric forms of subdomains can be exploited, various patterns of the physical solution can be captured using different numerical schemes in corresponding subdomains and the resulting subproblems can be solved on independently. DD has been extensively studied and applied. We refer the reader to [8] for an extensive description.

In this paper the following strategy is proposed: the given domain is split into sub-domains and the linear advection-diffusion Partial Differential Equation is discretised on each sub-domain using Finite Element Method (FEM) [10]; solutions from adjacent domains are forced to agree on the interface (the common boundary for adjacent domains) introducing an algebraic constraint. This generates a Differential Algebraic Equation (DAE) that describes the evolution of the FEM models and contains uncertain but bounded input modelling the error introduced by FEM. Assuming the availability of the observations of the pollutant concentration in the form of noisy sensor readings, the minimax state estimation approach [4], [1], [5] is applied to estimate the state of the DAE. The latter is accomplished by applying the generalised Kalman duality principle proposed in [9].

It is important to notice that DD by means of FEM can introduce artificial numerical instabilities. Namely, the stiffness matrix associated to each subdomain contains entries corresponding to the integrals over the interfaces. Those integrals are approximated by expansion of the solution using FEM, a finite linear combination of the chosen ba-

sis functions with unknown coefficients that is substituted into the integrals instead of the exact solution. Since that expansion has non-stationary coefficients, it follows that the corresponding entries in the stiffness matrix represent time dependent boundary conditions over the interface. In practice, for a finite number of elements, this might lead to instabilities in the stiffness matrix for each subdomain as pointed later in section II. On the contrary, the stiffness matrix associated with the entire domain has no such entries and hence no such instabilities. This artificial instability is compensated in this work by the well-known stabilizing effect of the minimax filter as suggested by the results of the numerical experiments in section III.

In [6] an approach similar to the one proposed in this work was introduced, combining DAE and DD but without the application of the filtering. Moreover, that work assumes the index of the DAE system to be 1, which is a hard constraint for the state estimation problems as it implicitly leads to differentiating the noise. In [2] the DD approach is also similar to the one in this work, but again there is no combination with filtering. Similarly to this work, continuity on the interfaces is required but that is done imposing Steklov Poincare equations, solved using an iterative procedure, on the interfaces.

B. Notation

$\mathbb{R}^n$ denotes the n-dimensional Euclidean space. Ω a domain in $\mathbb{R}^2$ and $\delta\Omega$ its boundary. $L^2([t_0, t_1], \mathbb{R}^n)$ denotes a space of square-integrable functions with values in $\mathbb{R}^n$. $H^1([t_0, t_1], \Omega)$ the Sobolev space of weak differentiable functions with support on Ω.

II. Problem Statement

Consider a linear transport problem on the domain $[t_0; t_1] \times \Omega$:

$$\begin{cases} \frac{\partial u}{\partial t} = Lu \\ u(0, x) = u_0(x) \\ u(t, x) = 0\,, \quad x \in \partial\Omega \end{cases} \tag{1}$$

where $\Omega \in \mathbb{R}^2$ is a bounded domain with Lipschitz boundary and the operator L is defined as follows:

$$L : H^1([t_0; t_1] \times \Omega) \to L^2([t_0; t_1] \times \Omega)$$

$$u \mapsto Lu = \mu \cdot \nabla u$$

and $u_0(x)$ is the initial condition reflecting the initial concentration. The homogeneous Dirichlet boundary condition reflects the assumption that domain Ω is chosen to be large enough to guarantee zero concentrations of u at $\partial\Omega$ which is the solution of choice in the civil engineering practice.

In the rest of this work (1) is referred to as the Global Problem. It is assumed that (1) is well-posed, that is it has a unique solution u_G for any initial condition u_0. To construct a numerical solution for the Global Problem DD is applied. In order to do that Ω is divided into N non-overlapping domains $\Omega_1, \ldots, \Omega_N$. Let $\Gamma_{i,j} = \partial\Omega_i \cap \partial\Omega_j$ denote the common boundary (interface) between the subdomains Ω_i, Ω_j, and let $\Gamma = \cup_{ij}\Gamma_{ij}$ denote the union of all interfaces. In addition, $\Gamma_{i,j}^{in}$, $\partial\Omega_i^{in}$ and $\Gamma_{i,j}^{out}$, $\partial\Omega_i^{out}$ stand for the parts of the boundary $\partial\Omega_i$ where the flow μ points inside Ω_i and outside Ω_i, respectively. In the next subsection the Global Problem is approximated by a set of Local Problems on each subdomain Ω_i. Hence the Global Problem is reconstructed via a set of Local Problems on each subdomain and with a continuity condition that enforces the continuity of the solution across the interface [8].

A. The Decomposed Problem

To illustrate the above, assume a Domain Decomposition of (1) in N subdomains. Consider the Local Problem i:

$$\begin{cases} \frac{\partial u_i}{\partial t} = L_i u_i \\ u_i(t, x) = 0, \text{ on } \partial\Omega^{in} \cap \partial\Omega_i^{in} \\ u_i(t, x) = u_j(t, x), \text{ on } \Gamma_{i,j}^{in} \\ u_i(0, x) = u_0(x) \end{cases} \tag{2}$$

and Local Problem j defined in the same fashion. It is also assumed that $\partial\Omega_i \cap \partial\Omega_j \neq \varnothing$. The operator L_i of the system (2) denotes the restriction of the operator L on subdomain Ω_i with the appropriate boundary condition provided $\partial\Omega_i \cap \partial\Omega \neq \varnothing$. The Local Problems i and j are said to be coupled if the fluid flow $\mu(x, y, t)$ points inwards both subdomains across the common boundary at the same time t. Otherwise, the Local Problems are said to be non-coupled and can be solved subsequently. However, it is realistic to assume that μ can change direction several times on the interface, making the Local Problems with common boundaries strictly coupled.

Let $B_{i,j} : \Omega_i \mapsto \Gamma_{ij}$ be a trace operator that assigns to $u \in H^1(\Omega)$ its value over the boundary of Ω Then, the Decomposed Problem can be described as follows:

$$\frac{\partial}{\partial t}\begin{pmatrix} u_1 \\ \vdots \\ u_N \end{pmatrix} = \begin{pmatrix} L_1 & \cdots & 0 \\ \vdots & \ddots & \vdots \\ 0 & \cdots & L_N \end{pmatrix}\begin{pmatrix} u_1 \\ \vdots \\ u_N \end{pmatrix} \tag{3}$$

with the set of continuity equations

$$Bu = \begin{pmatrix} B_{1,1} & \cdots & B_{1,N} \\ \vdots & \ddots & \vdots \\ B_{M,1} & \cdots & B_{M,N} \end{pmatrix}\begin{pmatrix} u_1 \\ \vdots \\ u_N \end{pmatrix} = 0 \tag{4}$$

and initial conditions

$$u_i(0, x) = u_i^0(x) \tag{5}$$

Note that the equation (4) enforces the continuity of the solution assembled from u_i across the interface Γ (see [8] for further details).

B. Finite Elements Approximation

In this work the discretization of the Global Problem (1) is obtained by means of the Finite Elements approximation. Namely, the function u_G is approximated by N_{nd} polynomial basis functions ϕ_i with compact support $u = \sum_{i=1}^{N_{nd}} u_i^G(t)\phi_i$. In FEM the coefficients of the discretization are computed

via a weak formulation of the Global Problem (1). Moreover, the weak formulation allows to incorporate boundary condition into a reduced model for the coefficients:

$$\begin{cases} M\frac{d\mathbf{u}}{dt} = S(t)\mathbf{u} \\ \mathbf{u}(0) = \mathbf{u}^0 \end{cases} \tag{6}$$

where $\mathbf{u} = (u_1^G(t)..u_N^G(t)^T$ represents the vector of the coefficients, M is the mass matrix, S is the stiffness matrix which also incorporates boundary conditions [10], and $\mathbf{u}^0$ is the projection of the initial condition. Further (6) is referred as the Discretized Global Problem. In the same way the i-th discretised Local Problem for the sub-domain Ω_i is defined as:

$$\begin{cases} M_i\frac{d\mathbf{u}_i}{dt} = S_i(t)\mathbf{u}_i \\ \mathbf{u}_i(0) = \mathbf{u}_i^0 \end{cases} \tag{7}$$

The discretised version of the Continuity equation (4) is given by:

$$B\mathbf{u} = 0 \tag{8}$$

where B is a matrix with elements in $\{-1, 0, 1\}$. In fact, (8) enforces solutions on adjacent sub-domains to coincide on the nodes of the common part of the FEM grid. The set of the N FEM Local Problems (7) with (8) forms a DAEs system which is further referred as Discretized Decomposed Problem. Solving the Discretised Decomposed Problems is equivalent to finding a solution of the system of DAE (7)-(8).

III. Main Results

In this section the Kalman Duality Principle, introduced in [9], is applied to Discretized Decompose Problem (7)-(8). In order to do that the following notation is introduced:

$$S = \begin{pmatrix} M_1^{-1}S_1 & \dots & 0 \\ \vdots & & \vdots \\ 0 & \dots & M_N^{-1}S_N \end{pmatrix}, F = \begin{pmatrix} I \\ 0 \end{pmatrix}, C = \begin{pmatrix} S \\ B \end{pmatrix}$$

$$\mathbf{a} = (u_1 \dots u_N)^T,\ \mathbf{e}_D = (e_1 \dots e_N)^T,\ \mathbf{a}_0 = (u_1^0 \dots u_N^0)^T$$

where $\mathbf{a}$ denotes the state vector and $\mathbf{a}_0$ is the initial condition. Define the error $\mathbf{e} = [\mathbf{e}_D; \mathbf{e}_A]'$, where the elements of $\mathbf{e}_A$ measure the difference between coefficients in the same node on a common boundary between subdomains. Similarly, $\mathbf{e}_D$ measures the model error that in introduced by the FEM discretisation. In similar fashion $\mathbf{e}_0$ is defined as the error related to the initial conditions $\mathbf{a}_0$.

The Discretised Decomposed Problem (7)-(8) can be written in a DAE form:

$$\frac{d}{dt}(F\mathbf{a}) = C\mathbf{a} + \mathbf{e},\ F\mathbf{a}(t_0) = \mathbf{a}_0 + \mathbf{e}_0\,, \tag{9}$$

where $\mathbf{e}_0$ and $\mathbf{e}$ are assumed to be inside the following ellipsoid:

$$\mathfrak{L} = \left\{ \mathbf{e} : \mathbf{e}_0 Q_0^T \mathbf{e}_0 + \int_{t_0}^{t_1} \mathbf{e}^T(t) Q(t) e(t) dt \le 1 \right\}, \tag{10}$$

with weighting matrices Q_0 and Q such that: $Q_0 = Q_0' > 0$ and Q^{-1}, $Q \in \mathbb{C}(t_0, t_1, \mathbb{R}^{m\times m})$, $Q(t) = Q'(t) > 0$. In fact, the ellipsoid defines the uncertainty in the system, introduced by FEM projection error.

Now, the goal is to find an estimate of a linear function $\ell(\mathbf{a}) = l^T F\mathbf{a}(t_1)$ with $\mathbf{a}$ solution of (9), in the class of linear functionals $u(y) := \int_{t_0}^{t_1} u^T(t)y(t)dt$ defined along the observations

$$y(t) = H(t)u(t) + \eta(t) \tag{11}$$

where $H(t)$ is an observation operator mapping the state vector $\mathbf{a}(t)$ to the space of the observed signal and η is the realization of a random process such that $E[\eta(t)] = 0$ and $E[\int_{t_0}^{t_1} \eta^T R^{-1}(t)\eta dt] \le 1,\ R^{-1}, R > 0 \in \mathbb{C}(t_0, t_1)$. The worst-case mean-squared estimation error is defined as follows: $\sigma(t_1, \ell, u) := \sup_{\mathbf{e}\in\mathfrak{L},\eta} E[(\ell(\mathbf{a}) - u(y))^2]$ and $\hat{u}$ minimizing σ for a given l is to be found (for more details the reader is referred to [9].

By using the Kalman Duality Principle of [9], $\hat{u}$ is found as $\hat{u} = RHp$, where p is the solution of the system:

$$\frac{d}{dt}(F'z) = -Cz + H^T RHp,\ F'z(t_1) = F'l \tag{12}$$

$$\frac{d}{dt}(Fp) = Cp + Q^{-1}z,\ Fp(t_0) = Q_0^{-1}z(t_0) \tag{13}$$

The vector z and the matrix Q are split according to the blocks S and B of matrix C:

$$z = \begin{pmatrix} z_s \\ z_b \end{pmatrix},\ Q^{-1} = \begin{pmatrix} Q_1 & Q_2 \\ Q_2^T & Q_4 \end{pmatrix} \tag{14}$$

Let set by definition:

$$M = S - Q_2Q_4^{-1}B,\ L = Q_1 - Q_2Q_4^{-1}Q_2^T \tag{15}$$

$$N = B_T Q_4^{-1} B + H^T RH \tag{16}$$

and $Q_4^{-1} = Q_4^{-1^T}$. The following Lemma can be proved.

Lemma 1: (12)-(13) is equivalent to the following ODE boundary value problem:

$$\begin{cases} \dot{z_s} = -M^T z_s + Np,\ z_s(t_1) = l_s \\ \dot{p} = Mp + Lz_s,\ p(t_0) = Q_0^{-1}z_s(t_0) \end{cases} \tag{17}$$

The proof is omitted for lack of space and it will be included in a future publication.

Now, using standard arguments from LQ control [7], a matrix K is to be found such that $p = Kz_s$. Inserting it into (17) the following equation is derived for K:

$$\dot{K}z_s = MKz_s + KM^T z_s - KNKz_s + Lz_s$$

$$K(t_0)z_s(t_0) = \widetilde{Q}_0^{-1} z_s(t_0)$$

Therefore K needs to satisfy the following Riccati equation:

$$\dot{K} = MK + KM^T - KNK + L,\ K(t_0) = \widetilde{Q}_0^{-1} \tag{18}$$

Assuming now that $K(t)$ solves (18) it is easy to see that z_s solves the equation $\dot{z_s} = -M^T z_s + NKz_s$, $z_s(t_1) = l_s$ and so $\hat{u} = RHKz_s$.

Finally, the equation for the minimax filter is introduced:

$$\dot{\hat{x}} = (M - KN)\,\hat{x} + KH^T Ry(t),\ \hat{x}(t_0) = 0 \tag{19}$$

and it is not hard to check that $\int_{t_0}^{t_1} u^T(t)y(t)dt = l_s^T\hat{x}(t_1)$ (Corollary 2.11 of [9]). Since this holds true for any l, it follows that $\hat{x}$ is the minimax estimate of the state vector of the DAE (9).

IV. Numerical Results

The feasibility of solving the Decomposed Problem (3)-(4)-(5) via (19) instead of the Global Problem (1) is addressed here by performing a set of numerical experiments that benchmark solutions of the Decomposed Problem versus solutions of the Global Problem.

A. FEM for the Decomposed Problem

While the projection using FEM of the Global Problem is strait forward and follows standard practises in FEM methodologies, its application to the Decomposed Problem can generate instabilities and inconsistencies. In order to overcome these difficulties a procedure that is the result of the theory demonstrated in this work is implemented and described in the following:

- FEM is applied to the Local Problems on the i non overlapping subdomains Ω_i, as in (2).
- The i FEM projections of the i Local Problems on Ω_i subdomains are made consistent on the interfaces by enforcing the continuity equation (8).
- The application of FEM and the continuity equation (8) is equivalent to finding solutions of the DAE Decomposed Problem (12)-(13).
- Since the DAE system is subject to uncertain FEM projection errors and the observations of the state are noisy, the Minimax filter is applied to estimate (17).
- (17) is benchmarked against the FEM Global Problem.

B. Numerical Experiments

Experiment 1 employs a trivial underlying flow, while Experiment 2 employs a complex underlying flow that is generated using the Environmental Fluid Dynamics Code (EFDC), a complex hydrodynamic model that is widely used in marine and coastal application [3]. For consistency the size of the subdomains is the same for both experiments, precisely 1000 meters by 1000 meters. It is assumed that initial conditions are non zero only in the first subdomain (the bottom left one) and are generated by a standard linear spline. Moreover, observations are present only in the first subdomain and only the first subdomain is activated at the beginning of both experiments. In both experiments the matrix Q that defines the control ellipsoid (10) needs to be constructed in order to minimise the algebraic error e_A and to constrain the model error e_D. Hence, Q is assumed block-decomposed due to the differential and algebraic part of equation (9):

$$Q = \begin{pmatrix} c_D I & 0 \\ 0 & c_A I \end{pmatrix} \tag{20}$$

with I the identity matrix and $c_D > 0$, $c_A > 0$. It is assumed that model error is relatively big, hence $c_D = 0.1$, while c_A is taken to be 10, 1000 or 10000 reflecting different levels of confidence in the continuity equation (8).

The minimax filter (19) is used in two different settings:

A Known initial condition with no observations. In this case the observation matrix H is set to be zero. Hence the second term in the (16) of Riccati equation and the term $K^T H^T R y(t)$ in the filter equation (19) are both zero. The inverse of Q_0 in (18) controls the norm ofthe error generated by the FEM projection of the initial conditions. This configuration can also be used when initial conditions contain noise.

B Unknown initial condition, but with available noisy observations. The observation matrix H becomes non trivial and the level of noise is described by the matrix R. Hence, the filter (19) has a nonzero term $K^T H^T R y(t)$ with zero initial conditions.

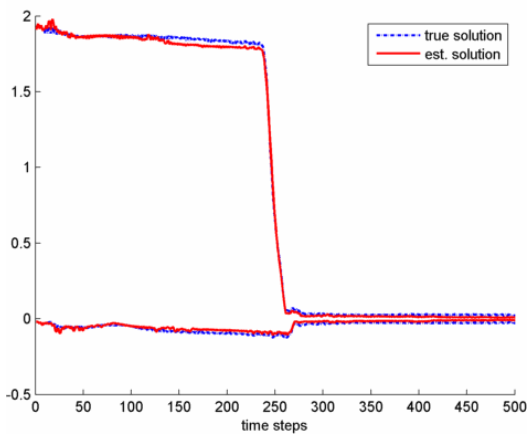

Fig. 1. max. and min. values of true solution and estimated solution over time of the problem with simple velocity field.

C. Experiment 1 Setting A

The underlying flow is described by the trivial velocity vector $\mu = [100; 0]$ and the global domain is decomposed into three subdomains along the horizontal axis. Solutions u_{est} of the minimax filter (19) are compared to the solutions u_{true} of the Discretised Global Problem (6). The discretization is done by using FEM configurations in which each subdomain is discretized with 35 by 35 finite elements and with $c_A = 10000$ in (20). Results are first shown in Figure 6, that shows the convergence after t = 300 of the max and min values of the estimated and true solutions.

The minimax estimation error at each time step is controlled by the Riccati matrix via

$$\ell^T (u_{true}(t) - u_{est}(t)) \leq [(K(t)\ell)^T \ell]^{\frac{1}{2}} \tag{21}$$

where ℓ is an arbitrary vector. Tracking the maximum eigenvalue of the Riccati Matrix shows (omitted here for lack of space) that it converges to a constant value proving that the minimax error is bounded.

In Figure 2 the norm of the algebraic constraint Bu is tracked over time. The two peaks in the graph correspond to the activation of the second and third subdomains: at activation time the values of the solution on the newly activated subdomain are identically zero as opposed to values of the solution correpsonding to the active subdomain. This explains the peaks which disappear right after the activation.

Experiment's configuration	FEM elements	c_A	$\|Bu\|$	$\|u_{true} - u_{est}\|$	$\|u_{est}\|$	$\frac{\|u_{true}-u_{est}\|}{\|u_{est}\|}$
Experiment 1.A	25 by 25	10	0.8826	8.2233	130.2418	0.0631
		1000	0.0837	7.6172	130.3710	0.0584
		10000	0.0484	7.3979	130.4357	0.0567
	35 by 35	10	0.8550	9.0107	181.2854	0.0497
		1000	0.0783	8.1814	181.4112	0.0451
		10000	0.1053	8.2472	181.4719	0.0454
Experiment 1.B: Observations sampled every 20, 10, 5 time steps (from top to bottom) (norms calculated over 105-500 time steps)	35 by 35	10000	0.0648	15.3839	131.0368	0.1174
		10000	0.0564	6.6893	136.1204	0.0491
		10000	0.0600	6.2483	136.3587	0.0458
Experiment 2.A	35 by 35	10	0.3418	12.3133	279.3252	0.0441
Experiment 2.B (norms over 300-600 time steps)	35 by 35	10	0.3748	16.3014	190.4613	0.0856

TABLE I

COMPARISON OF NORMS FOR DIFFERENT NUMBERS OF FEM ELEMENTS AND c_A

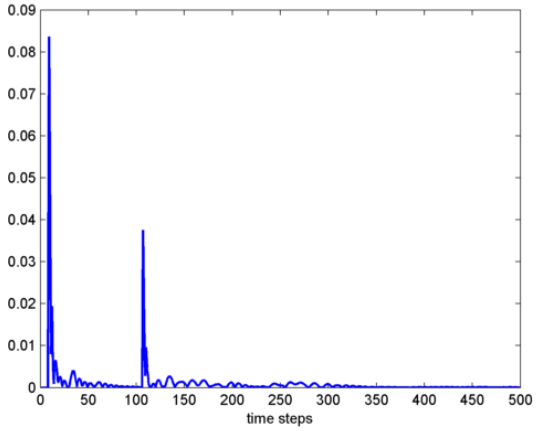

Fig. 2. $\|Bu\|$ for the problem with simple velocity field.

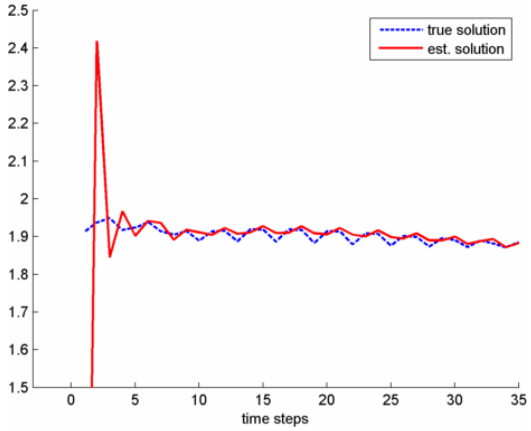

Fig. 3. max. values of estimated and true solutions over first 35 time steps of the problem with simple velocity field. Estimated solution assimilates observations every time step.

The same experiment was made for few more configurations as reported in table I where norms are defined as $\|u\| = \sum \|u(t_n)\|^2_{\mathbb{R}^N}$. From the table a correspondence between small values of $\|Bu\|$ and the estimation error can be noticed. The same can be concluded about the number of FEM elements and the estimation error (more FEM, less error), due to the fact that a higher number of elements over the subdomain means a higher number of elements near the boundaries. The latter are the zones where $\mathbf{e}_A$ controls the error in the continuity equation. As a result enforcing low $\mathbf{e}_A$ makes the solution of the Discretised Decomposed Problem to better approximate the solution od the Discretised Global Problem.

D. Experiment 1 Setting B

Here the underlying flow field and Domain Decomposition is the same as above. Observations are generated by restricting u_{true} on the first subdomain. Moreover, since $R = 1000 \cdot I$ it follows that the system is supposed to give a lot of weight to the observations. The estimated solution converges to the true solution rather quickly as it can be seen in figure 3. The corresponding rows in the Table I allow to reach the same conclusions as in the previous setting: the decrease in the norm of Bu corresponds to the decrease of the estimation error. Moreover, the same behavior is observed when more observations are added, increasing their frequency brings an improvement of the estimation error. It is noted that while in Experiment 1A there were no observations, the algebraic part of DAE (9) could be considered as the observation equation. Since the pair (S, B) is not observable (there can be different initial conditions for the corresponding FEM model leading to solutions which are in the null-space of B), it follows that the algebraic part of DAE does not lead to decrease in the eigen values of the Riccati matrix representing the level of the uncertainty in the system. On the other hand, by adding actual observations a decrease of the maximal eigenvalue of the Riccati matrix is observed.

E. Experiment 2 Setting A

For the second test the underlying flow field was generated by EFDC. The global domain is decomposed in 2 by 2 subdomains, discretized using 35 by 35 finite elements and the initial conditions are generated in the same way as in Experiment 1 Setting A. Results are shown in Figure 4, in which the max and min values of the estimated and true solutions are plotted over time. In Figure 5 the norm at each time step of the algebraic constraint Bu is tracked. Compared to Experiment 1 the behavior of the algebraic constraint is

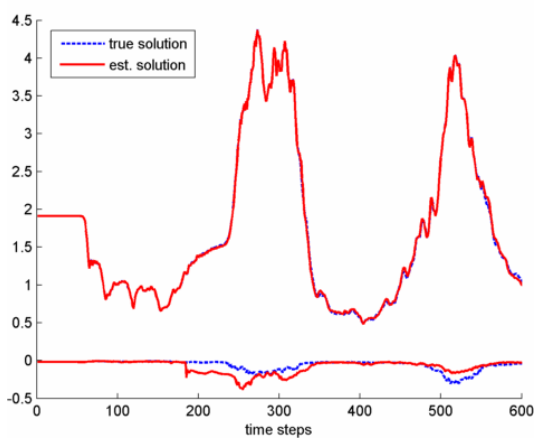

Fig. 4. max. and min. values of true solution and estimated solution over time of the problem with EFDC generated velocity field.

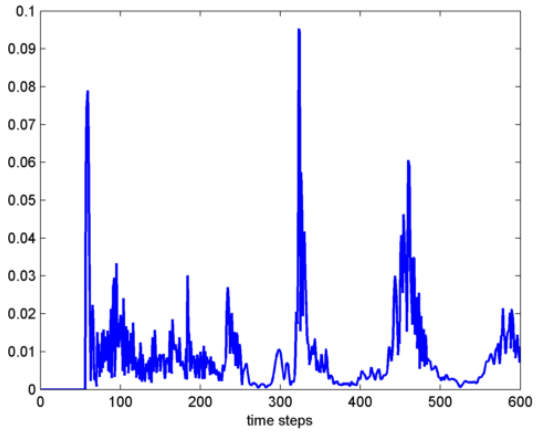

Fig. 5. $\|Bu\|$ over time for the problem with EFDC generated velocity field.

much more complex, demonstrating that the concentrations cross the boundaries between the subdomains a few times.

Note that the reason for the discrepancies in the time window 200-300 in figure 4 is due to the simultaneous activation of three subdomains almost at the same time step.

F. Experiment 2 Settings B

Here, as in Experiment 1B, initial conditions are unknown but observations are available. Those are generated by restricting u_{true} on the first subdomain (bottom left), sampling it every 5 time-steps and adding to it normally distributed noise in the interval $[0, 0.1]$. $[0, 0.1]$.

Results are first shown in Figure 6, in which the max and min values of the estimated and true solutions are plotted over time. The figure shows the convergence after $t = 300$ of the max and min values of the estimated and true solutions. Note that for the simple fluid flow taken in the Experiment 1 the corresponding stiffness matrix is stationary and stable in Lyapunov sense. In the present experiment the fluid flow is non-stationary and exhibits a complex behavior that together with FEM approximation error amounts to the non-stationary

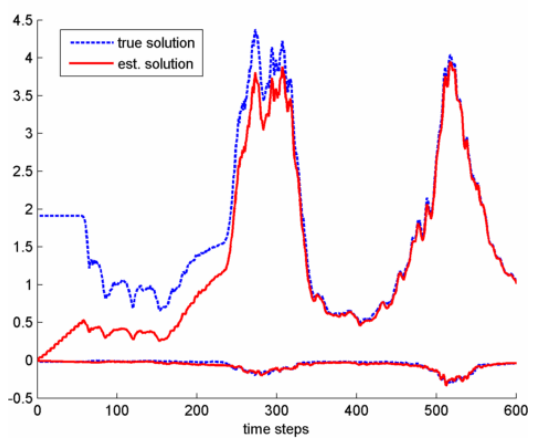

Fig. 6. max. and min. values of true solution and estimated solution over time of the problem with EFDC generated velocity field. Estimated solution assimilates observations sampled every 5 time steps.

stiffness matrix with positive eigen-values. This artificial instability is resolved by the minimax filter which injects the stabilizing feed-back into the state equation.

V. Conclusion

In Domain Decomposition the non stationary nature of the problems treated can lead over time to an accumulation of the error introduced by the space discretisation. In the case of the transport system treated here, integrations over long time windows can lead to high degree of inaccuracy when there is a complex underlying flow field. The introduction of a minimax filtering technique in this work helps to control this error and to maintain the solution within a control ellipsoid, by tuning the parameters within the minimax filter. Last but not least, the introduction of a filter allows the coupling of observations with the solutions of the transport equation.

References

[1] F. L. Chernousko. *State Estimation for Dynamic Systems*. Boca Raton, FL: CRC, 1994.

[2] Lucia Gastaldi. A domain decomposition for the trasport equation. *Contemporary Mathematics*, 157, 1994.

[3] John Hamrick. A three-dimensional environmental fluid dynamics computer code: Theoretical and computational aspects. *Special Report in Applied Marine Science and Ocean Engineering, Virginia Institute of Marine Science, College of William & Mary, Gloucester Point, Virginia*, 317, 1992.

[4] Alexander Kurzhanski and István Vályi. *Ellipsoidal calculus for estimation and control*. Systems & Control: Foundations & Applications. Birkhäuser Boston Inc., Boston, MA, 1997.

[5] A. Nakonechny. A minimax estimate for functionals of the solutions of operator equations. *Arch. Math. (Brno)*, 14(1):55–59, 1978.

[6] K.D. Nakshatrala, K.B. Hjelmstad and D.A. Tortorelli. A feti-based domain decomposition technique for time-dependent first-order systems based on a dae approach. *International Journal For Numerical Methods In Engineering*, 75:1385–1415, 2008.

[7] T. Reid. *Riccati differential equations*. Academic press, 1972.

[8] A. Toselli and O. Widlund. *Domain Decomposition Methods*. Springer, 2004.

[9] S. Zhuk. Kalman duality principle for a class of ill-posed minimax control problems with linear differential-algebraic constraints. *Applied Mathematics & Optimisation*, 2012. under revision.

[10] O. C. Zienkiewicz, R. L. Taylor, and J. Z. Zhu. *The Finite Element Method: Its Basis and Fundamentals*. Butterworth-Heinemann, 2005.